Version of Record: https://www.sciencedirect.com/science/article/pii/S0040609019306261
Manuscript_eae0f03a2f0f3b021d85518dbf73dc50

Doping of TiO_2 nanotubes with nitrogen by annealing in ammonia for visible light activation: influence of pre- and post-annealing in air

Andjelika Bjelajac[a, *, 1], Rada Petrović[b], Maja Popović[c], Zlatko Rakočević[c], Gabriel Socol[d], Ion N. Mihailescu[d], Djordje Janaćković[b]

[a]University of Belgrade, Innovation center of Faculty of Technology and Metallurgy, Karnegijeva 4, 11000 Belgrade, Serbia

[b]University of Belgrade, Faculty of Technology and Metallurgy, Karnegijeva 4,11000 Belgrade, Serbia

[c]Vinča Institute of Nuclear Sciences, University of Belgrade, P.O. Box 522, 11001 Belgrade, Serbia

[d]National Institute for Lasers, Plasma, and Radiation Physics, Lasers Department, "Laser-Surface-Plasma Interactions" Laboratory, PO Box MG-54, RO-77125, Magurele, Ilfov, Romania

[*]Corresponding author: tel: + 381 11 3303741.
E-mail address: abjelajac@tmf.bg.ac.rs (A. Bjelajac).
[1]Present address: LPICM, Ecole Polytechnique, CNRS, IP Paris, Route de Saclay, 91128 Palaiseau, France

Abstract

The ~60 nm wide and ~2 μm long TiO_2 nanotubes were obtained by anodization of Ti films sputtered on F-doped tin oxide glass. For N-doping the samples were annealed in ammonia atmosphere. The effect of pre- and post-annealing in air on the nature and amount of incorporated N was studied by X-ray photoelectron spectroscopy. By measuring the absorption spectra of the obtained samples and interpreting the corresponding Tauc plots it was shown that the sample annealed just in ammonia showed the highest visible light absorption even after sputtering cleaning and a decrease of N amount from 3.8 % to 1 %. Pre and/or post annealing in air led to smaller amount of incorporated N, that caused less pronounced absorption enhancement and smaller band gap narrowing compared to the sample annealed only in ammonia. By fitting of N 1s line, the contribution that was assigned to substitutional N was detected only in the samples that did not sustained post-annealing. The study showed that post-annealing in air might lead to partial conversion of N atoms in TiO_2 to oxidized nitrogen species that are easily removed with sputtering. It is also possible that substitutional nitrogen was suppressed by oxygen from air to move to interstitial site. Weakly bonded NO_x surface species, which are cleaned away by sputtering, can be removed by post-annealing in air. Those surface species could act as sensitizers and when their amounts are reduced, the core absorption properties, as a result of interstitial incorporation of N in TiO_2 structure, were revealed. Much lower visible light sensitization was achieved in the case of pre-annealed sample in comparison to sample without pre-annealing, regardless the same quantity and type of incorporated nitrogen.

Keywords: Titania; Nanotubes; Nitrogen doping; Thermal annealing; X-ray photoelectron spectroscopy; Diffuse reflectance spectroscopy; Band gap

1. Introduction

Titanium dioxide (TiO_2) is one of the most studied semiconductor due to its wide application ranging from gas sensing [1], water photoelectrolysis [2], photocatalysis [3], biocoatings [4] and solar cells [5], which are all an effect of the photosensitivity of titania. However the optical properties of titania are limited by its absorption edge at 387 nm for anatase or 413 nm for rutile phase [6], which is only ~5 % of entire solar spectrum. In order to improve photo response of titania, two methods are widely applied: the morphology modification and the doping of TiO_2. It is already shown that one-dimensional nanotubular structure has superior characteristics compared to nanoparticular TiO_2, in terms of electron propagation within the structure upon UV radiation. It is proved that diffusion of electrons is 30 times faster along 1D TiO_2 nanotubes (NTs) than through nanoparticles [7]. Also, in TiO_2 NTs the electron transfer loss is reduced since there are no grain boundaries as it is the case with nanoparticles [8]. For obtaining TiO_2 NTs, the anodization technique has been applied as it is a feasible and reproducible method for controlled synthesis of highly ordered TiO_2 NTs arrays [9]. Herein, the anodization of Ti sputtered on F-doped tin oxide (FTO) glass was performed, since such obtained photoanode is transparent and can be used in front side illumination configuration of a solar cell. The front side illumination mode provides

higher efficiency of the solar cell when compared with the solar cell consisting of TiO_2 NTs film on Ti foil support (back side illumination mode) [10],[11].

Another approach that provides the enhancement of TiO_2 absorbance properties is doping, where N-doping is headmost. The previous studies showed that N doping of TiO_2 NTs can be done by immersing of the NTs in N containing solutions [12], thermal treatment in NH_3 gas atmosphere [13], using N-containing Ti alloys obtained by an arc-melting [14], high-energetic ion implantation [15], adding urea [16] or NH_4NO_3[17] in the electrolyte for anodization. Since the TiO_2 NTs synthesized via anodization technique are amorphous, it is necessary to anneal them at T > 250 °C [18] in order to transform to more conductive crystalline structure. For N doping the method of our choice was annealing in NH_3 at 450 °C in order to obtain anatase phase of TiO_2 [19]. Our previous study showed that N-doping of TiO_2 via annealing in NH_3 was more effective, meaning higher amount of N was incorporated if TiO_2 was amorphous rather than if TiO_2 was crystalline as obtained by pre-annealing in air. However, this study was about nanoparticular TiO_2 synthetized via sol-gel method not by anodization as proposed here [20]. Furthermore, it was important to investigate the effect of post-annealing on the N-doped TiO_2 NTs and their optical properties. Nitridation (NH_3 treatment) of TiO_2 not only leads to nitrogen doping but also to the formation of defects including oxygen vacancies and Ti^{3+} states, which are all contributing to visible light absorption features. Oxygen vacancies and Ti^{3+} states were reported to strongly influence photocatalytic activity by acting as charge carriers trapping and/or recombination centers by themselves or through a impurity–vacancy electronic interaction [21]. Chen et al. reported that post-annealing in O_2 of NH_3-treated TiO_2 leads

to the removal of surface amino species that consequently enhances the photocatalytic activity by adsorption of oxygen and formation of $O_2^{\bullet -}$ radicals, which are important for benzene degradation. In the mentioned research they analysed the N-doping and post-annealing effect on P25 Degussa. Apart from decrease of oxygen vacancies number, they have also showed that by post-annealing the surface Ti^{3+} defects were decreased and the separation of photogenerated carriers was improved [22]. However, they also proved that post-annealing treatment caused the decrease of visible light activation of N-TiO_2, which suggested that oxygen vacancies are not responsible for the visible light activity. Another study [23] about NH_3 treated nanopartucular TiO_2 obtained by a sol-gel method also presented the positive effect of the post-annealing in air on photocatalytic oxidation of ethylene. The discussion was about surface hydroxyl groups that react with photogenerated holes producing active hydroxyl radicals which are important for photocatalysis. Additionally, surface hydroxyl groups can act as surface sites for adsorbing organic molecules that also capture photogenerated holes. The trapping of holes stabilizes photogenerated electron–hole pairs, improving photocatalytic efficiency. In the study they explained that due to the nitridation process numerous NH_3 react with hydroxyl groups on the TiO_2 surface leading to decrease of the number of surface sites accessible for reactants and resulting in low photocatalytic activity. With post-annealing most of the NH_3 was removed and provided a higher density of surface hydroxyl groups for adsorbing organic substrates as well as capturing photogenerated holes, thereby stabilizing the charge carriers of the sample. What is more, they showed that post-annealing stabilizes N atoms in TiO_2 lattice. Therefore, we found it important to investigate if and how the annealing in air prior and/or after the

annealing in NH_3 would affect the amount and type of N incorporation in TiO_2 structure and how would that further impact the optical properties of the N doped TiO_2.

There are only few studies related to anodized TiO_2 NTs films treated in NH_3 for N doping [13, 16, 24, 25]. Even less, only one reported the investigation of FTO supported TiO_2 NTs obtained by anodization [26]. The majority of studies investigated the use of Ti foil to produce double-wall and single-wall TiO_2 NTs that were annealed in NH_3[27]. But there is no study about the pre or post treatment in air of the TiO_2 NTs film. Vitiello et al. [28] mentioned that their TiO_2 NTs on Ti support were re-annealed at 450 °C for 1 h and that lead to lower photocurrent in the visible light. They indicate that diffusional loss of N in non-nitrogen containing environments is possible. However, the detailed studied was not provided. Another study of Lemes et al. [29] was about optimization of nitridation temperature for efficient N doping also on TiO_2 NTs on Ti foil. A morphology change resulting in partial closure of the NTs at 500 °C annealing was noticed. This was related to the density difference that occurs due to nitrogen doping and hence material exhibit different density after nitridation as compared to its starting oxide material. Within this work we have also investigated how the pre and post annealing with NH_3 treatment can influence the morphology of the NTs. In order to preserve the open-porosity for better performances as photoanode in solar cell, the annealing temperature for the present study was chosen to be 450 °C. The high temperature interval was just 30 min, since it was previously reported that prolongation of NH_3 treatment led to smaller amount of incorporated N in TiO_2 NTs [30].

2. Experiment

Pure titanium thin films were deposited by radio frequency magnetron sputtering (RF-MS) onto FTO glass (PI-KEM Ltd, 200 nm FTO film, 12-14 Ω/cm^2) using titanium target (Alfa Aesar GmbH). The FTO substrates were ultrasonically cleaned successively in acetone, ethanol and deionizated water for 10 min in an ultrasonic bath before being mechanically fixed inside the deposition chamber at a 40 mm target-to-substrate separation distance. Prior to deposition a shadow mask was applied on the FTO glass substrate such as to obtain a coated area of 10 x 10 mm^2 in the sample centre. The films were sputtered using a Cesar RF Power Generator with a Dressler RMC-1 Matching Controller (13.56 MHz) deposition system having a magnetron cathode with a plasma ring of ~50 mm diameter. The sputtering chamber was first evacuated down to a base pressure of ~2 x 10^{-4} Pa. Then pure argon was admitted in the reactor chamber at constant gas flow rate of 5 sccm. The sputtering was carried out at room temperature for 1 h at a working pressure and RF power of 0.5 Pa and 60 W, respectively. The conditions were chosen to obtain well-adhered films with a homogeneous nanostructured surface, that will provide highly ordered and alighted TiO_2 NTs [3]. It was previously reported that increase of substrate temperature and/or RF power or the pressure produced bigger grains and higher roughness of the films [32], [33].

The sputtered titanium films were anodized in ethylene glycol (EG) containing 0.3 wt% ammonium fluoride and 2 wt% water, using platinum as cathode. The electrodes were kept 20 mm apart and the voltage was set at 60 V. The transparent films were obtained after 10 min of anodization, whereupon the samples were well rinsed with water and let

to dry in air for 24 h. The dried samples were then annealed in air alone (the sample was labelled as TiO_2-air) or in air followed by annealing in ammonia (TiO_2-Air/NH_3) or just in ammonia (TiO_2-NH_3) or in ammonia then in air (TiO_2-NH_3/Air) or first in air, then in ammonia and finally in air again (TiO_2-Air/NH_3/Air). All the annealing processes were performed at 450 °C for 30 min with a heating rate of 8 °C/min and in all cases the cooling was natural till reaching room temperature.

The surface morphology of the samples was studied using a Tescan Mira X3 field emission scanning electron microscope (FESEM). The diffused reflectance spectra (DRS) of the pristine undoped and doped TiO_2 NTs formed on FTO glasses were recorded using a Shimadzu 2600 UV-Vis spectrophotometer with an integrating sphere attachment in the wavelength range from 300 to 750 nm.

The X-ray photoelectron spectroscopy (XPS) was used for the composition analysis and the chemical bond identification of N-doped TiO_2 films. XPS analyses were carried out on a SPECS customized Ultra-High Vacuum surface analysis system containing sputter ion gun, PHOIBOS 100 spectrometer for energy analysis, dual anode Al/Ag monochromatic source and an electron flood gun. High resolution XPS spectra were taken using monochromatic Al Kα line (photon energy of 1486.74 eV) with the electron pass energy of 20 eV, the energy step of 0.1 eV and the dwell time of 1-2 s depending on the photoelectron line intensity. Sample sputter cleaning was performed using 3 keV Ar^+ ion beam at a 45° incident angle. The sputtering duration was only 1 min in order to reduce the preferential sputtering effects which typically, in the case of TiO_x samples,

reduce 'x'. The sputtered surface was 5x5 mm^2, and the typical ion beam current was around 5 μA.

Quantitative composition analysis was performed from the relative intensities of the characteristic photoelectron lines, determined as an area below a line after subtracting Shirley background, using atomic sensitivity factors provided by the manufacturer. The detailed analysis of the photoelectron lines was performed based on the following peak model: each contribution was fitted to a pseudo-Voigt GL(30) peak profile; half widths of peaks in the frame of the same line is considered to be equal; the intensity ratio of Ti 2p spin-orbit doublet peaks attributed to the same chemical bond was fixed to the theoretical value 1:2. Binding energy axis correction due to the charging effects was based on the position of the main C 1s line contribution, assuming it corresponds to the adventitious carbon situated at 284.8 eV.

3. Results and discussion

Fig. 1 presents the overview of the FESEM micrograph of the as-anodized TiO_2 NTs with a length of ~2 μm and ~60 nm inner diameter. The morphology of NTs corresponds to previously reported double-wall NTs that are expected for the NTs formed using EG based electrolyte for anodization. By using SEM the distinction

between outer and inner layers is not very apparent [34]. The tubes seem mainly to consist of a thick tube wall that is tapered from top to bottom (Fig 1a)).

Fig 1.

Fig. 2 shows the FESEM micrographs of TiO_2 NTs after annealing. It can be seen that in all cases the open porosity of the NTs remained, which is an important feature of the structure, having a high specific surface area.

Fig. 2

The survey wide-energy XPS spectra were taken for all samples annealed in ammonia in order to identify and quantify present elements. In all cases, the characteristic Ti 2p, O 1s, C 1s and Sn 3d lines were detected as well as N 1s line of a small intensity. Fig. 3 shows a representative XPS spectrum of the TiO_2-Air/NH_3 sample. Ti and O originate from TiO_2 film, whereas Sn signal comes from the F-SnO_2 film beneath (FTO glass). C was expected as a usual constituent of surface contaminants.

Fig. 3

The chemical composition before (i) and after (ii) sputtering of all the samples annealed in ammonia is given in Table 1. It can be seen that in all samples, the amount of C is high (12- 20 %) and that it is not significantly decreased after ionic sputtering (except

for the TiO_2-NH_3 sample). This means that sputtering removes only the impurities from the top surface of the NTs, but not from the NTs' wall in depth. The amount of N before and after sputtering remains mostly the same, except for the TiO_2-NH_3 sample, where N concentration decreases from 3.8 % to 1.0 % [26]. In our previous study [26] we assumed that in this case the major amount of N was bonded (adsorbed) to the surface via weak bonds, enabling easy removal by sputtering. Further investigation about the effect of post-annealing in air (sample TiO_2-NH_3/Air), showed that the concentration of N is much smaller (0.7 %) than in the sample TiO_2-NH_3, but it does not change after the sputtering. This indicates that in this sample N was uniformly incorporated along the depth of TiO_2 NTs creating stronger bonds. It can be supposed that the N that was removed by sputtering from the surface of TiO_2-NH_3 is the same type as the N removed by the post-calcination in air for obtaining the TiO_2-NH_3/Air sample. Similar occurrence can be observed comparing the samples TiO_2-Air/NH_3 and TiO_2-Air/NH_3/Air, except that the N concentration in TiO_2-Air/NH_3 (1.4 %) was much smaller than in the sample TiO_2-NH_3 and sputtering does not reduce it significantly (1.3 %). Therefore, it can be concluded that in well crystalline TiO_2 (due to annealing in air) a very small amount of N is bonded to the surface via weak bonds, thus the sputtering did not affect much to the N concentration. It seems that the post-annealing in air of the TiO_2-Air/NH_3 sample (sample TiO_2-Air/NH_3/Air) enabled the removal of all weakly bonded N, as there was no difference in N concentration after the sputtering (0.8 %).

Table 1.

The fitting results for the N 1s line before (i) and after (ii) the sputtering of the samples TiO_2-NH_3, TiO_2-NH_3/Air, TiO_2-Air/NH_3, TiO_2-Air/NH_3/Air are given in Table 2. The results for TiO_2-NH_3 sample were already discussed in our previous study [26], but they are repeated within the given table for easier comparison with the new results.

Table 2.

Firstly noticed from Table 2, is that in comparison to TiO_2-NH_3 the sample TiO_2-NH_3/Air lost the contributions ascribed as the peak 1 and 2 of the N 1s line and that the peak 4 appeared instead. The peak 1 is characteristic for substutionally incorporated N [26] and the peak 2 is associated to chemisorbed N (from N_2 or NH_3) [35]. On the other hand, the peak 4 at 402.10 eV is accociated to surface adsorbed NO_x species [16]. This results implies that post-annealing in air caused partial conversion of N atoms in TiO_2-NH_3 to oxidized nitrogen species that are easily removed with sputtering [23]. It is also possible that surface adsorbed NH_3 (peak 2) were oxidized to NO_x species (peak 4). The other contribution of N in case of the TiO_2-NH_3/Air sample is the peak 3 at 400.08 eV, that corresponds to interstitially incorporated N [36] and it was only one detected after sputtering (it coincides to the resulting spectrum presented in Fig. 4 as envelope). Another assumption can be made since the formation energy of interstitial N in TiO_2 lattice is lower than for substitutional [37], the substitutional N might be suppressed by oxygen from air to move to interstitial site. Analysing whole Table 2, it can be noticed that there is always more interstitional N than substitutional no matter if the pre or post annealing was performed. This means that formation of N-Ti-O bonds is more favourable until certain saturation when excessive N atoms start to form N-Ti-N bonds

[38]. The reported saturation limit is 1.5 % and coincides with the amount of incorporated N for the samples TiO_2-NH_3 and TiO_2-Air/NH_3 (Table 1) where both interstitional and substitutional N were detected.

Fig. 4

For further analysis of the TiO_2-Air/NH_3 sample, N 1s line was fitted in three contributions both before and after sputtering (Fig. 4). Apart from the peak at ~ 400 eV, that corresponds to interstitial N (N_{inter}) and the peak at ~ 402 eV, associated to NO_x species adsorbed at the surface, there is also the peak at ~ 396 eV, which is assigned to substitutional incorporation of N (N_{subs}) [28, 36] as in the case of TiO_2-NH_3 [26]. The contribution at ~ 402 eV decreases after sputtering that indicates to weakly bonded NO_x species (Table 2). Proportionally to the decrease of the peak 4, the two remeaining peaks 1 and 3 increased. However, the ratio N_{inter}:N_{subs} before sputtering was 1.63 whereas after it decreased to 1.33 (Table 2), which suggested that the incorporation of both substitutaional and interstitial nitrogen was not uniform along the NTs.

In the case of TiO_2-Air/NH_3/Air before sputtering the three contribution of the N 1s line are also deduced from the fitting (Fig. 4), as for the TiO_2-Air/NH_3 sample, however the contribution at ~ 396 eV is smaller than for the TiO_2-Air/NH_3 sample. The N_{inter}:N_{subs} ratio before sputtering is much bigger (5.25) than for the sample without post-annealing. This proves that the amount of substitutional N decreases due to the post-annealing in air. It was already discussed that it might be due to suppression of oxygen from air to move substitutional N to interstitial sites. However, sputtering caused the total loss of

the N_{subs}. This agrees with the assumption that incorporation of both N_{inter} and N_{subs} is not uniform along the NTs. The peak 3 coincides with the resulting spectrum (envelope).

To deduce the influence of type of N-doping (calcination of amorphous or crystalline TiO_2 in NH_3), post-annealing in air and ion sputtering on optical properties of the obtained film, DRS spectra were recorded, using a bare FTO glass for baseline. The samples were analyzed before and after the XPS measurement, meaning before and after ionic sputtering. Together with the DRS spectra, the Tauc plots of the squared root of the Kubelka-Munk functions ($F(R) = (1- R)^2/(2R)$) versus photon energy were given for the estimation of the corresponding band gaps. Fig. 5 illustrates that the TiO_2-NH_3 sample had the highest absorption in the visible region. However, it showed a big declination of absorption due to sputtering. This is in accordance with XPS results, having in mind that the amount of N in this sample decreased from 3.8 % to 1.0 % and showing that some surface attached species are removed by sputtering. Obviously, high content of surface attached species causes high absorption in the visible region of the sample TiO_2-NH_3. The visible light absorption of the sample after sputtering is mainly due to the presence of substitutional and interstitial N, meaning that the sputtering revealed the intrinsic property of the sample. Therefore, although the sample TiO_2-NH_3 has a very narrow band gap before sputtering (1.63 eV), the value obtained after sputtering, 2.86 eV, can be considered as more realistic. Actually the first slope of the Tauc plot with the tangent line at 3.06 eV reveals the contribution of the substitutional N, but the overall impact on the absorption properties comes from the second slope that corresponds to the interstitial N [24], [39]. Besides the substitutional and interstitial

incorporation of N, we proved that NH_3 treatment led to pronounced diffusion of Sn in TiO_2 from FTO support [40]. Therefore, the band gap narrowing is surely affected by Sn incorporation as well. In the case of TiO_2-NH_3, Sn concentration is the highest among the samples (Table 1) and it decreases from 4.7 to 4.0 after sputtering, which can also influence the lower band bap narrowing than before sputtering.

When analyzing the sample TiO_2-NH_3/Air, it can be noticed that it possesses absorption in the visible light region similar as the sample TiO_2-NH_3 after sputtering. Since it did not show any substitutional N, this result proves the strong effect of interstitial N. Considering the effect of sputtering on the TiO_2-NH_3/Air sample, it can be seen that the absorption remained almost the same, which agrees with the XPS data that the amount of N did not change after sputtering. Also, the interpreted band gaps values before and after sputtering, 2.83 eV and 2.96 eV, respectively, are close. By comparing DRS spectra of TiO_2-NH_3 and TiO_2-NH_3/Air, it is obvious that strong visible-light harvesting of the TiO_2-NH_3 sample is a result of the presence of species which are removed by post-annealing in air or by spattering. These species are not important for the practical application of the N-TiO_2 NTs photoanode and can be removed by post-annealing in air.

Similar as in the case of TiO_2-NH_3 sample, the surface species amount in the sample TiO_2-Air/NH_3 declined after sputtering with the increase of substitutional N contribution. The sputtering effect was the most vivid for the sample TiO_2-Air/NH_3 where it revealed the three absorption shoulders, originating from three different N contributions. The first add-on shoulder can be a consequence of substitutionally incorporated N, the next two are originating from interstitial N and surface trapped NO_x

species. Consequently, the interpretation of the Tauc plot gave three values of band gap. The sample TiO_2-Air/NH_3/Air showed the smallest visible-light absorption and a negligible band gap narrowing (3.27 eV and 3.24 eV before and after sputtering, respectively) compared to the undoped sample. A small add-on shoulder was observed after sputtering, when only interstitial N was detected. When compare to the sample TiO_2-NH_3/Air which also possess only interstitial N, it can be concluded that the pre-treatment in air, which led to crystalline structure, enable only a shallow level states caused by incorporated N [24], whereas direct annealing in NH_3 causes deeper level states [41]. What is more the pre-treatment in air hinders the creation of oxygen vacancies that benefit to visible light photo-response. Even though there was 0.8 % of N detected in the TiO_2-Air/NH_3/Air it did not lead to significant visible light sensitization.

Fig. 5

4. Conclusions

TiO_2 NTs, obtained by anodization of Ti films sputtered on FTO glass, were doped with nitrogen by annealing in ammonia atmosphere. The effect of pre- and post-annealing in air on the nature and amount of incorporated N was studied by XPS technique. SEM analyses of the films proved that the nanotubular structure remained open irrespective of the type of annealing treatment. The analysis of the N 1s XPS spectra showed that, in all cases, N was incorporated interstitially in TiO_2 structure, while substitutional incorporation of N was detected only in the samples that did not

sustain post-annealing in air. Weakly bonded NO_x species, which are removed by ionic spattering, can be partially removed from the surface by post-annealing. It was assumed that substitutional nitrogen was suppressed by oxygen from air during post-annealing to move to interstitial site. In addition, it is possible that post-annealing led to partial conversion of N in TiO_2 lattice to oxidized nitrogen species, that are easily removed with sputtering. The visible-light activation of N-doped samples was studies by analyzing DRS spectra and corresponding Tauc plots. The sample annealed just in ammonia showed the highest absorption in the visible region, even after sputtering cleaning and decrease of N amount from 3.8 % to 1 %. Pre- and/or post-annealing in air led to smaller amount of N, that caused less pronounced absorption enhancement compared to the sample annealed only in ammonia. The surface species that were removed by sputtering, as well as post-annealing, could act as sensitizers and when their amounts are reduced, the core absorption properties were revealed. Pre-annealing in air, which led to the crystalline structure before N-doping, provided much lower visible light sensitization than N-doping of amorphous TiO_2, regardless the same quantity and type of incorporated nitrogen.

Acknowledgements

The Serbian authors acknowledge with thanks the financial support of the Ministry of Education, Science and Technological Development, Republic of Serbia through the Projects III 45019, III 45005. A.B. is grateful to the program "Start up for science 2016"

organized by the Centre for leadership development, Serbia that helped her to conduct herein studies.

The Romanian authors acknowledge with thanks the partial financial support of this work by UEFISCDI under the contract ID 304/2011.

References

[1] V. Galstyan, E. Comini, G. Faglia, G. Sberveglieri, TiO_2 nanotubes: recent advances in synthesis and gas sensing properties., Sensors (Basel) 13 (2013) 14813–38. doi:10.3390/s131114813.

[2] K. Shankar, G. K. Mor, H. E. Prakasam, S. Yoriya, M. Paulose, O. K. Varghese, C. A. Grimes, Nanotube arrays up to 220 μm in length: Use in water photoelectrolysis and dye-sensitized solar cells, Nanotechnology 18 (2007) 065707. doi:10.1088/0957-4484/18/6/065707.

[3] A. Fujishima, T. N. Rao, D. A. Tryk, Titanium dioxide photocatalysis, J. Photochem. Photobiol. C Photochem. Rev. 1 (2000) 1–21. doi:10.1016/S1389-5567(00)00002-2.

[4] K. S. Brammer, S. Oh, C. J. Cobb, L. M. Bjursten, H. Van Der Heyde, S. Jin, Improved bone-forming functionality on diameter-controlled TiO_2 nanotube surface, Acta Biomater. 5 (2009) 3215–3223. doi:10.1016/j.actbio.2009.05.008.

[5] B. O'Regan, M. Grätzel, A low-cost, high-efficiency solar cell based on dye-sensitized colloidal TiO_2 films, Nature. 353 (1991) 737–740.

[6] D. A. H. Hanaor, C. C. Sorrell, Review of the anatase to rutile phase

transformation, J. Mater. Sci. 46 (2011) 855–874. doi:10.1007/s10853-010-5113-0.

[7] P. Roy, S. Berger, P. Schmuki, TiO_2 nanotubes: Synthesis and applications, Angew. Chemie - Int. Ed. 50 (2011) 2904–2939. doi:10.1002/anie.201001374.

[8] D. R. Baker, P. V. Kamat, Photosensitization of TiO_2 nanostructures with CdS quantum dots: Particulate versus tubular support architectures, Adv. Funct. Mater. 19 (2009) 805–811. doi:10.1002/adfm.200801173.

[9] C. A. Grimes, G. K. Mor, TiO_2 Nanotube Arrays Synthesis, Properties, and Applications, Springer Berlin Heidelberg, 2009.

[10] G. K. Mor, O. K. Varghese, M. Paulose, C. A. Grimes, Transparent highly ordered TiO_2 nanotube arrays via anodization of titanium thin films, Adv. Funct. Mater. 15 (2005) 1291–1296. doi:10.1002/adfm.200500096.

[11] D.-J. Yang, H. Park, S.-J. Cho, H.-G. Kim, W.-Y. Choi, TiO_2-nanotube-based dye-sensitized solar cells fabricated by an efficient anodic oxidation for high surface area, J. Phys. Chem. Solids. 69 (2008) 1272–1275. doi:10.1016/j.jpcs.2007.10.107.

[12] H. Wu, Z. Zhang, High photoelectrochemical water splitting performance on nitrogen doped double-wall TiO_2 nanotube array electrodes, Int. J. Hydrogen Energy. 36 (2011) 13481–13487. doi:10.1016/j.ijhydene.2011.08.014.

[13] H. Li, J. Li, Y. Wang, L.Wang, Preparation and Characterization of the Highly Regular Nitrogen Doped Anatase TiO_2 Nanotube, Mater. Sci. Forum. 749 (2013) 654–659. doi:10.4028/www.scientific.net/msf.749.654.

[14] D. Kim, S. Fujimoto, P. Schmuki, H. Tsuchiya, Nitrogen doped anodic TiO_2 nanotubes grown from nitrogen-containing Ti alloys, Electrochem. Commun. 10

(2008) 910–913. doi:10.1016/j.elecom.2008.04.001.

[15] A. Ghicov, J. M. Macak, H. Tsuchiya, J. Kunze, V. Haeublein, L. Frey, P. Schmuki, Ion implantation and annealing for an efficient N-doping of TiO_2 nanotubes, Nano Lett. 6 (2006) 1080–1082. doi:10.1021/nl0600979.

[16] R. P. Antony, T. Mathews, P. K. Ajikumar, D. N. Krishna, S. Dash, A. K. Tyagi, Electrochemically synthesized visible light absorbing vertically aligned N-doped TiO_2 nanotube array films, Mater. Res. Bull. 47 (2012) 4491–4497. doi:10.1016/j.materresbull.2012.09.061.

[17] K. Shankar, K.C. Tep, G.K. Mor, C. A. Grimes, An electrochemical strategy to incorporate nitrogen in nanostructured TiO_2 thin films: modification of bandgap and photoelectrochemical properties, J. Phys. D. Appl. Phys. 39 (2006) 2361–2366. doi:10.1088/0022-3727/39/11/008.

[18] A. Tighineanu, T. Ruff, S. Albu, R. Hahn, P. Schmuki, Conductivity of TiO_2 nanotubes: Influence of annealing time and temperature, Chem. Phys. Lett. 494 (2010) 260–263. doi:10.1016/j.cplett.2010.06.022.

[19] C. Di Valentin, G. Pacchioni, A. Selloni, Origin of the different photoactivity of N-doped anatase and rutile TiO_2, Phys. Rev. B - Condens. Matter Mater. Phys. 70 (2004) 1–4. doi:10.1103/PhysRevB.70.085116.

[20] A.J. Albrbar, V. Djokić, A. Bjelajac, J. Kovač, J. Ćirković, M. Mitrić, D. Janaćković, R. Petrović, Visible-light active mesoporous, nanocrystalline N,S-doped and co-doped titania photocatalysts synthesized by non-hydrolytic sol-gel route, Ceram. Int. 42 (2016) 16718–16728. doi:10.1016/j.ceramint.2016.07.144.

[21] Z. Zhang, X. Wang, J. Long, Q. Gu, Z. Ding, X. Fu, Nitrogen-doped titanium dioxide visible light photocatalyst: Spectroscopic identification of photoactive

centers, J. Catal. 276 (2010) 201–214. doi:10.1016/j.jcat.2010.07.033.

[22] Y. Chen, X. Cao, B. Lin, B. Gao, Origin of the visible-light photoactivity of NH_3-treated TiO_2: Effect of nitrogen doping and oxygen vacancies, Appl. Surf. Sci. 264 (2013) 845–852. doi:10.1016/j.apsusc.2012.10.160.

[23] X. Chen, X. Wang, Y. Hou, J. Huang, L. Wu, X. Fu, The effect of postnitridation annealing on the surface property and photocatalytic performance of N-doped TiO_2 under visible light irradiation, J. Catal. 255 (2008) 59–67. doi:10.1016/j.jcat.2008.01.025.

[24] M. Zhang, K. Yin, Z. D. Hood, Z. Bi, C. A. Bridges, S. Dai, Y. S. Meng, M. P. Paranthaman, M. Chi, In situ TEM observation of the electrochemical lithiation of N-doped anatase TiO_2 nanotubes as anodes for lithium-ion batteries, J. Mater. Chem. A. 5 (2017) 20651–20657. doi:10.1039/c7ta05877b.

[25] S. S. Park, S. M. Eom, M. Anpo, D. H. Seo, Y. Jeon, Y. G. Shul, N-doped anodic titania nanotube arrays for hydrogen production, Korean J. Chem. Eng. 28 (2011) 1196–1199. doi:10.1007/s11814-010-0498-7.

[26] A. Bjelajac, V. Djokić, R. Petrović, N. Bundaleski, G. Socol, I.N. Mihailescu, Z. Rakočević, D. Janaćković, Absorption boost of TiO_2 nanotubes by doping with N and sensitization with CdS quantum dots, Ceram. Int. 43 (2017) 15040–15046. doi:10.1016/j.ceramint.2017.08.029.

[27] S. A. Al-Thabaiti, R. Hahn, N. Liu, R. Kirchgeorg, S. So, P. Schmuki, S. N. Basahel, S. M. Bawaked, NH_3 treatment of TiO_2 nanotubes: from N-doping to semimetallic conductivity, Chem. Commun. 50 (2014) 7960. doi:10.1039/c4cc02069c.

[28] R. P. Vitiello, J. M. Macak, A. Ghicov, H. Tsuchiya, L.F.P. Dick, P. Schmuki, N-

Doping of anodic TiO_2 nanotubes using heat treatment in ammonia, Electrochem. Commun. 8 (2006) 544–548. doi:10.1016/j.elecom.2006.01.023.

[29] T. Lemes, S. Khan, E. Leal da Silva, L. L. de Costa, S. R. Teixeira, C. Aguzzoli, C. F. Malfatti, Effect of nitridation temperature on TiO_2 nanotubular structure and its photoelectrochemical performance, Renew. Energy Power Qual. J. 1 (2018) 778–781. doi:10.24084/repqj16.466.

[30] J. Vujančević, P. Andričević, A. Bjelajac, V. Đokić, M. Popović, Z. Rakočević, E. Horváth, M. Kollár, B. Náfrádi, A. Schiller, K. Domanski, L. Forró, V. Pavlović, Đ. Janaćković, Dry-pressed anodized titania nanotube/$CH_3NH_3PbI_3$ single crystal heterojunctions: The beneficial role of N doping, Ceram. Int. 45 (2019) 10013–10020. doi:10.1016/j.ceramint.2019.02.045.

[31] A. Bjelajac, V. Djokic, R. Petrovic, G. E. Stan, G. Socol, G. Popescu-Pelin, I. N. Mihailescu, D. Janackovic, Pulsed laser deposition method for fabrication of CdS/TiO_2 and PbS photoelectrodes for solar energy application, Dig. J. Nanomater. Biostructures. 10 (2015) 1411–1418.

[32] V. Chawla, R. Jayaganthan, A. K. Chawla, R. Chandra, Microstructural characterizations of magnetron sputtered Ti films on glass substrate, J. Mater. Process. Technol. 209 (2009) 3444–3451. doi:10.1016/j.jmatprotec.2008.08.004.

[33] Z. Aznilinda, S. H. Herman, R. A. Bakar, M. Rusop, Physical characteristic of room-temperature deposited Ti thin films by RF magnetron sputtering at different RF power, 2012 10th IEEE Int. Conf. Semicond. Electron. ICSE 2012 - Proc. (2012) 328–332. doi:10.1109/SMElec.2012.6417152.

[34] H. Mirabolghasemi, N. Liu, K. Lee, P. Schmuki, Formation of “single walled” TiO_2 nanotubes with significantly enhanced electronic properties for higher

efficiency dye-sensitized solar cells, Chem. Commun. 49 (2013) 2067–2069. doi:10.1039/c3cc38793c.

[35] S. H. Kang, H. S. Kim, J. Y. Kim, Y. E. Sung, Enhanced photocurrent of nitrogen-doped TiO_2 film for dye-sensitized solar cells, Mater. Chem. Phys. 124 (2010) 422–426. doi:10.1016/j.matchemphys.2010.06.059.

[36] T. Lin, C. Yang, Z. Wang, H. Yin, X. Lü, F. Huang, J. Lin, X. Xie, M. Jiang, Effective nonmetal incorporation in black titania with enhanced solar energy utilization, Energy Environ. Sci. 7 (2014) 967–972. doi:10.1039/c3ee42708k.

[37] Z. Zhao, Q. Liu, Mechanism of higher photocatalytic activity of anatase TiO_2 doped with nitrogen under visible-light irradiation from density functional theory calculation, J. Phys. D. Appl. Phys. 41 (2008) 25105–25114. doi:10.1088/0022-3727/41/2/025105.

[38] H. Wang, Y. Yang, J. Wei, L. Le, Y. Liu, C. Pan, P. Fang, R. Xiong, J. Shi, Effective photocatalytic properties of N doped titanium dioxide nanotube arrays prepared by anodization, React. Kinet. Mech. Catal. 106 (2012) 341–353. doi:10.1007/s11144-012-0439-z.

[39] H. Abdullah, M. M. R. Khan, H. R. Ong, Z. Yaakob, Modified TiO_2 photocatalyst for CO_2 photocatalytic reduction: An overview, J. CO_2 Util. 22 (2017) 15–32. doi:10.1016/j.jcou.2017.08.004.

[40] A. Bjelajac, R. Petrović, V. Djokic, V. Matolin, M. Vondraček, K. Dembele, S. Moldovan, O. Ersen, G. Socol, I.N. Mihailescu, D. Janaćković, Enhanced absorption of TiO_2 nanotubes by N-doping and CdS quantum dots sensitization: Insight into the structure, RSC Adv. 8 (2018) 35073–35082. doi:10.1039/c8ra06341a.

[41] S. Sato, R. Nakamura, S. Abe, Visible-light sensitization of TiO_2 photocatalysts by wet-method N doping, Appl. Catal. A Gen. 284 (2005) 131–137. doi:10.1016/j.apcata.2005.01.028.

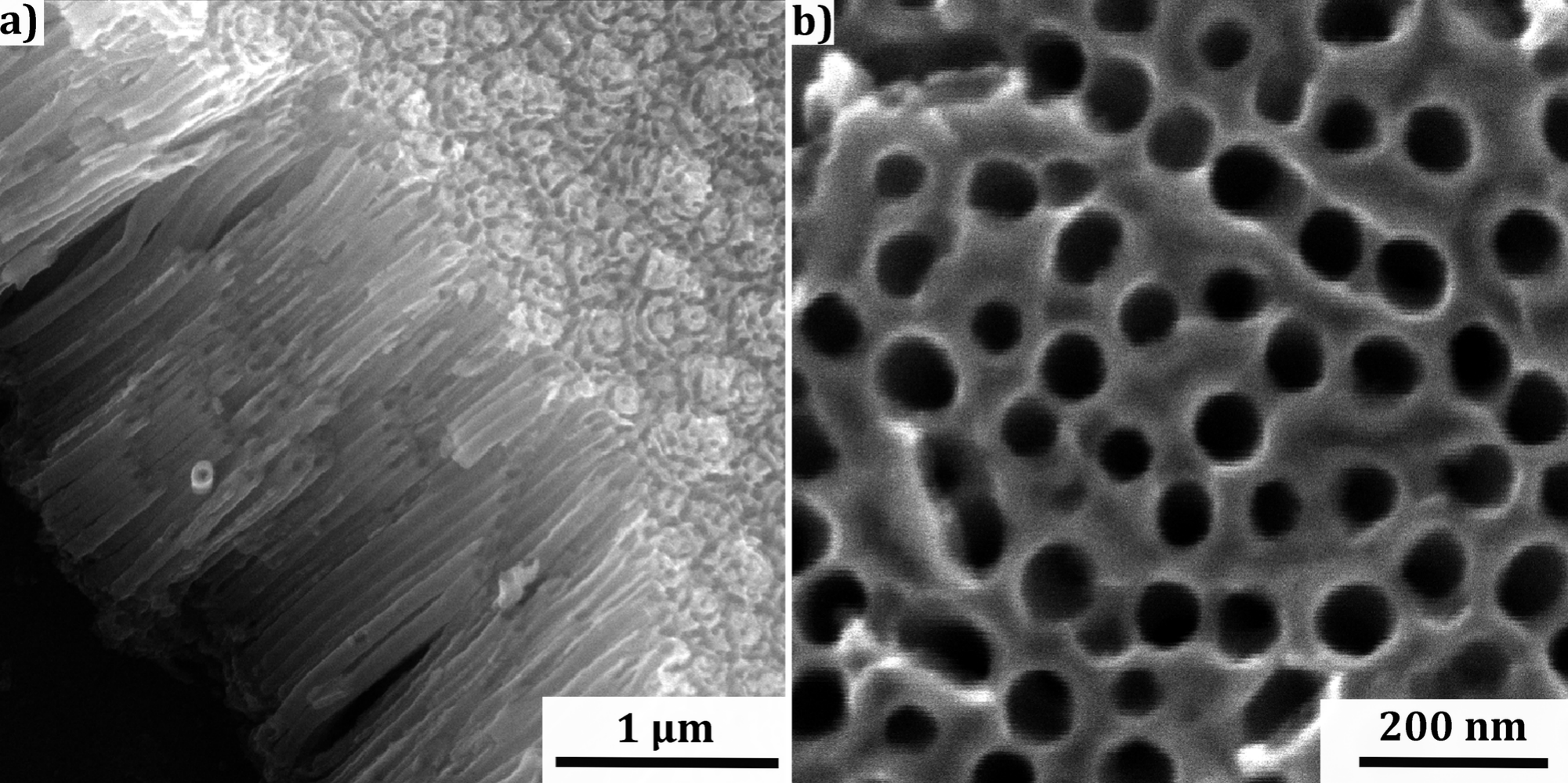
a)
1 µm
b)
200 nm

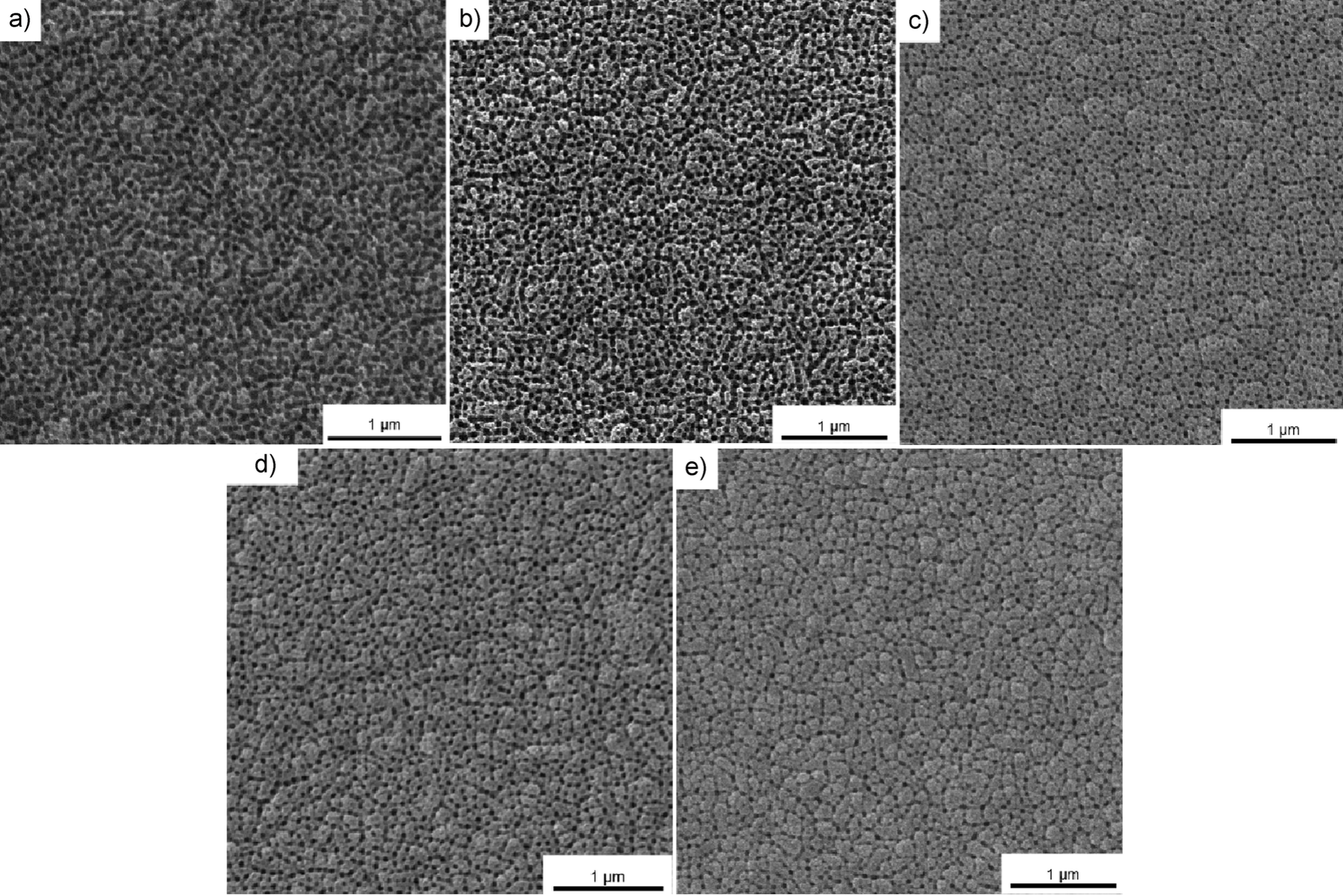
a)
1 µm
b)
1 µm
c)
1 µm
d)
1 µm
e)
1 µm

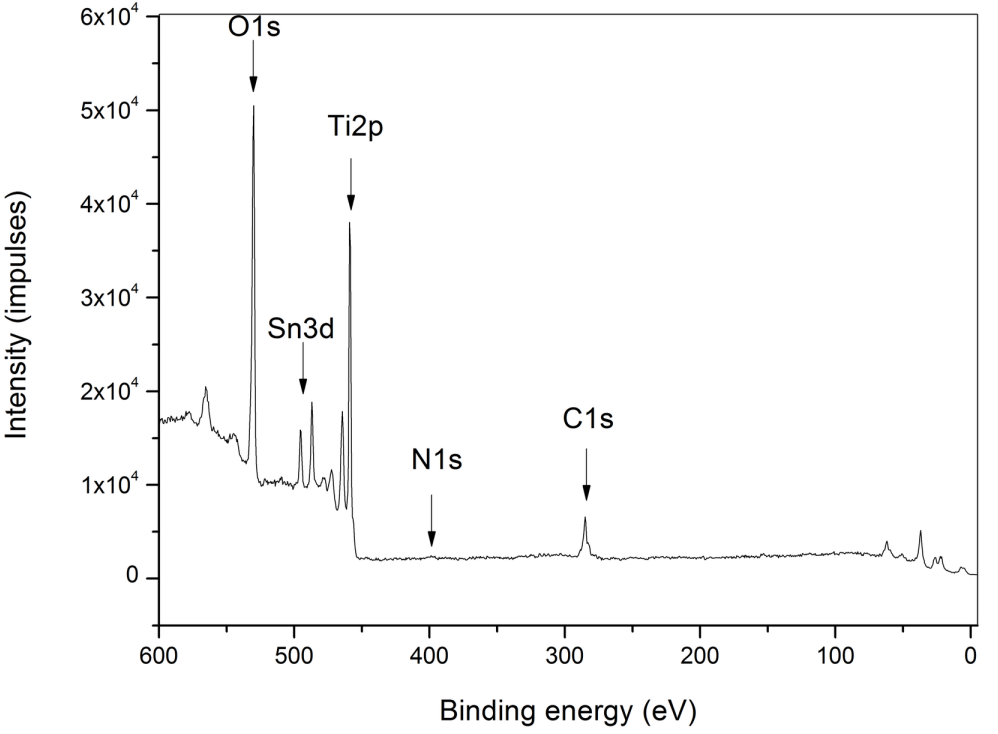
6x10^4
5x10^4
4x10^4
3x10^4
2x10^4
1x10^4
0
Intensity (impulses)
O1s
Ti2p
Sn3d
N1s
C1s
600
500
400
300
200
100
0
Binding energy (eV)

Before ionic sputtering

After ionic sputtering

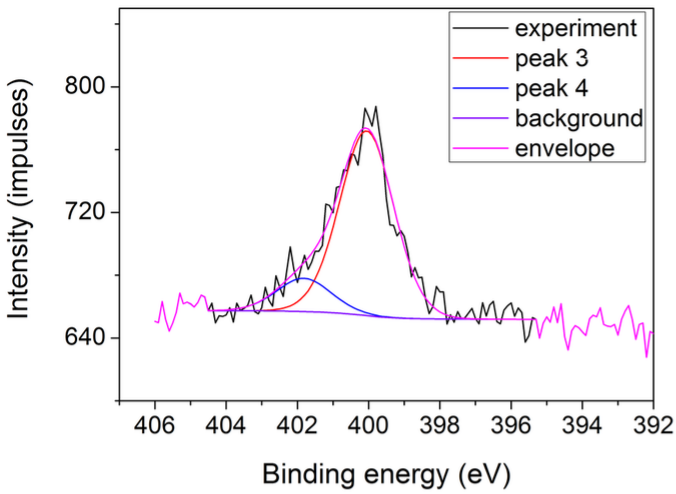

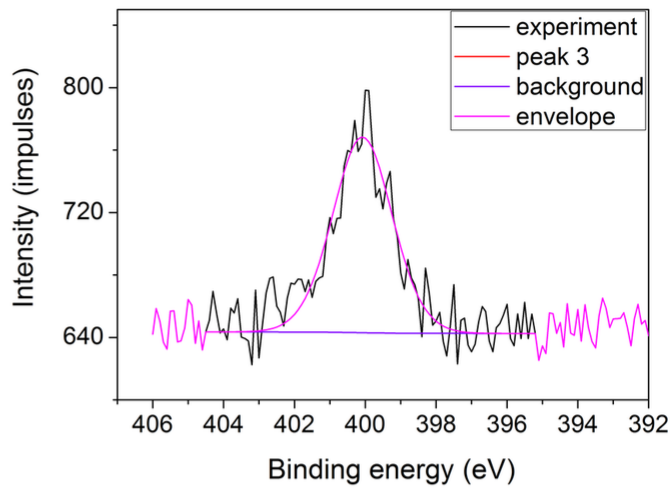

TiO_2-NH_3/Air

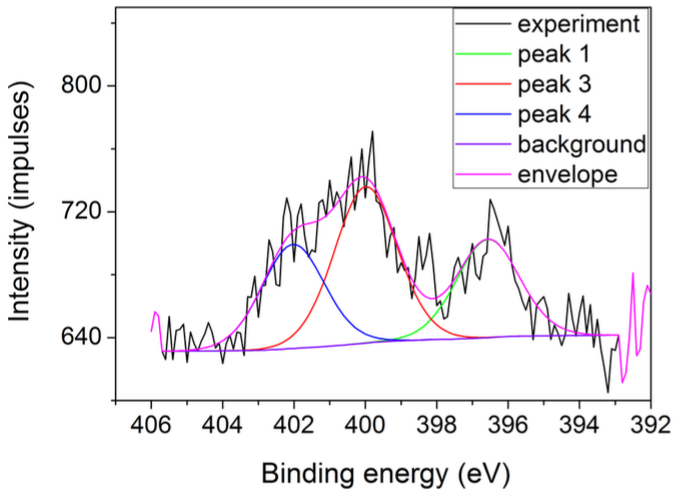

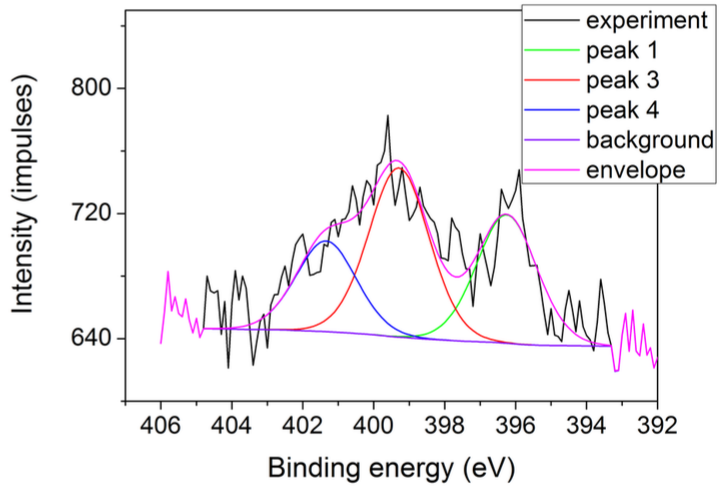

TiO_2-Air/NH_3

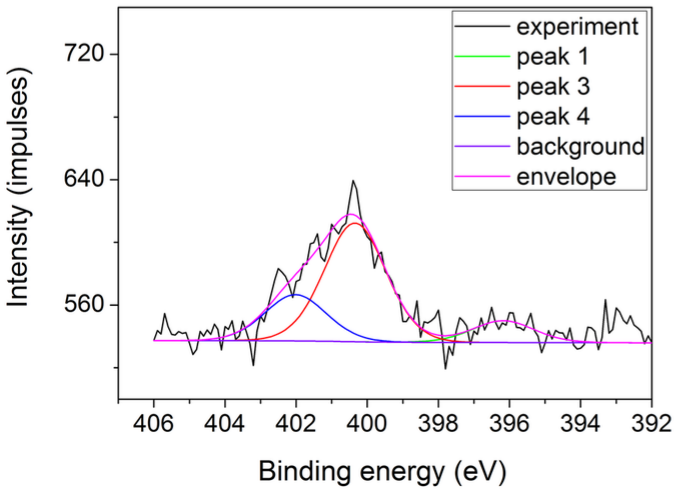

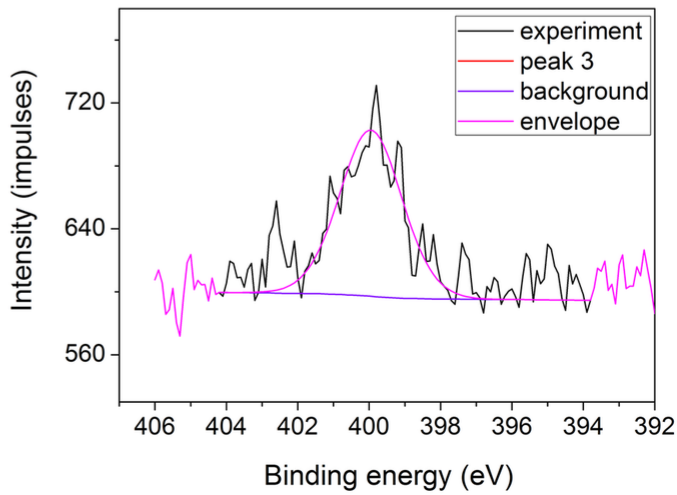

TiO_2-Air/NH_3/Air

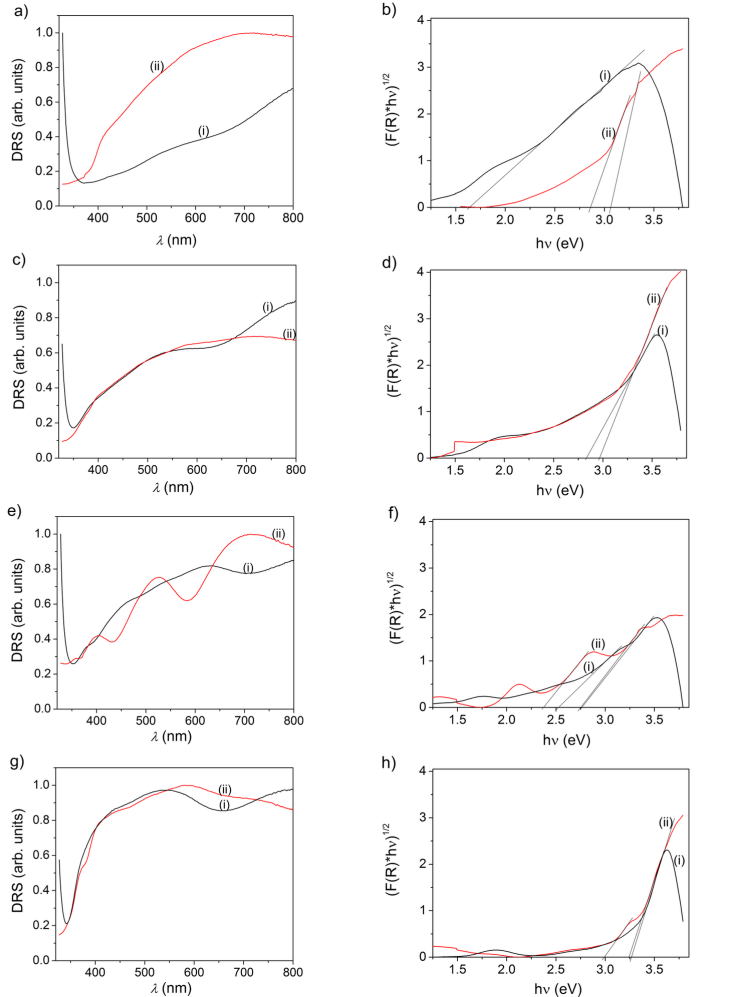
a)
DRS (arb. units)
λ (nm)
(i)
(ii)
b)
(F(R)*hν)^1/2
hν (eV)
(i)
(ii)
c)
DRS (arb. units)
λ (nm)
(i)
(ii)
d)
(F(R)*hν)^1/2
hν (eV)
(ii)
(i)
e)
DRS (arb. units)
λ (nm)
(ii)
(i)
f)
(F(R)*hν)^1/2
hν (eV)
(ii)
(i)
g)
DRS (arb. units)
λ (nm)
(ii)
(i)
h)
(F(R)*hν)^1/2
hν (eV)
(ii)
(i)

Table 1. Chemical composition of the surface of the analyzed TiO_2 films before (i) and after (ii) sputtering

Sample	Sputtering	C (%)	N (%)	O (%)	Ti (%)	Sn (%)
TiO_2-NH_3 [22]	(i)	20.7	3.8	53.1	17.7	4.7
	(ii)	6.2	1.0	62.6	26.2	4.0
TiO_2-NH_3/Air	(i)	15.0	0.7	58.5	22.2	3.6
	(ii)	12.2	0.7	60.5	23.0	3.5
TiO_2-Air/NH_3	(i)	20.5	1.4	54.6	20.0	3.5
	(ii)	17.7	1.3	55.9	21.6	3.4
TiO_2-Air/NH_3/Air	(i)	16.6	0.8	59.2	20.9	2.3
	(ii)	15.3	0.8	59.5	21.7	2.7

Table 2. The fitting results for the N 1s line before (i) and after (ii) sputtering

Sample	Sputtering	Peak 1 (position/%)	Peak 2	Peak 3	Peak 4
TiO_2-NH_3[22]	(i)	396.1 eV/4%	398.7 eV/52 %	400.4 eV/44 %	
	(ii)	396.6 eV/26 %	398.6 eV/33 %	400.2 eV/41 %	
TiO_2-NH_3/Air	(i)			400.08 eV/85%	402.10 eV/15 %
	(ii)			400.08 eV/100 %	
TiO_2-Air/NH_3	(i)	396.56 eV/27 %		399.99 eV/44 %	402.02 eV/29 %
	(ii)	396.25 eV/33 %		399.29 eV/44 %	401.34 eV/23 %
TiO_2-Air/NH_3/Air	(i)	396.18 eV/12 %		400.34 eV/63 %	402.01 eV/25 %
	(ii)			399.97 eV/100 %	